Evaluation of Tsunami Loads on Wood-Frame Walls at Full Scale

David Linton[1]; Rakesh Gupta, M.ASCE[2]; Dan Cox, M.ASCE[3]; John van de Lindt, M.ASCE[4]; Mary Elizabeth Oshnack[5]; and Milo Clauson[6]

Abstract: The performance of full-scale light-frame wood walls subjected to wave loading was examined using the Large Wave Flume of the Network for Earthquake Engineering (NEES) Tsunami Facility at Oregon State University. The hydrodynamic conditions (water level and bore speed) and structural response (horizontal force, pressure, and deflection) were observed for a range of incident tsunami heights and for several wood wall framing configurations. The walls were tested at the same cross-shore location with a dry-bed condition. For each tsunami wave height tested, the force and pressure profiles showed a transient peak force followed by a period of sustained quasi-static force. The ratio of the transient force to quasi-static force was 2.2. These experimental values were compared with the predicted values using the linear momentum equation, and it was found that the equation predicted the measured forces on the vertical wall within an accuracy of approximately 20% without using a momentum correction coefficient. The experiments also showed that the more flexible 2×4 wall resulted in lower peak forces when compared with 2×6 walls subjected to similar tsunami heights. However, the 2×6 walls were able to withstand larger waves before failure.
DOI: 10.1061/(ASCE)ST.1943-541X.0000644.

CE Database subject headings: Tsunamis; Impact forces; Frames; Wood structures; Walls.

Author keywords: Tsunami forces; Light-frame wood walls; Impact; Tsunami damage; Tsunami mitigation.

Introduction

The recent earthquake and subsequent tsunami that devastated Japan in March 2011 and the December 2004 Indian Ocean tsunami that caused severe damage and loss of life to numerous coastal communities underscore the need for a better understanding of tsunami-structure interaction. These events, along with several recent smaller tsunamis, have further reminded the world of the vulnerability of coastal communities during tsunami events. Prior to the most recent disaster, little research has focused on tsunami-structure interaction. Most of the previous knowledge was from field reconnaissance (Lukkunaprasit and Ruangrassamee 2008) or small-scale laboratory experiments (e.g., Cross 1967; Ramsden 1996; Lukkunaprasit et al. 2009). Several experiments have been conducted on small-scale vertical walls with regular or random waves, but large-scale tsunami loading has been limited (Arikawa 2009). Approximately 95% of buildings in the United States use light-frame wood construction. For this reason, the experiments in this study focus on investigating full-scale wood-frame wall performance, force, and pressure data for solitary waves similar to those that occur during a tsunami. This paper presents the methodology and results of a large-scale experimental program for tsunami waves on wooden vertical walls in the Large Wave Flume of the Network for Earthquake Engineering (NEES) Tsunami Facility at Oregon State University. The purpose of this work was to investigate how a flexible structure performs when subjected to a solitary wave bore and compare the measured forces with predictive equations from the literature. The specific objectives were

- To evaluate the linear momentum equation developed for steady-flow assumptions and determine whether the force coefficient C_f developed by Cross (1967) is necessary, and
- To observe the performance of light-frame wood walls during a tsunami event.

Numerous studies have been conducted on the generation and propagation of tsunamis across the ocean. However, research on the inundation and subsequent impact of tsunamis on structures is less common. For many years, research has been conducted on wave forces on vertical walls, but most of these experiments have been conducted on a small scale. Ramsden (1996) focused on the impact of translator waves (bores and dry-bed surges) on a vertical wall on a small scale rather than breaking waves on a large scale. The measured forces and moments in Ramsden's study should only be used in relation to sliding and overturning because they are not applicable to punching failures. Also tested on a small scale were several scale-model houses. Thusyanthan and Madabhushi (2008) investigated the effects of openings and anchorage on force and pressure for a 1:25-scale model house. Wilson et al. (2009) developed an understanding of the nature of wave loading on a wood-framed scale residential building model for a variety of building configurations and test conditions. Testing was performed on a one-sixth-scale

[1]Former Graduate Research Assistant, School of Civil and Construction Engineering and Dept. of Wood Science and Engineering, Oregon State Univ., Corvallis, OR 97331.

[2]Professor, Dept. of Wood Science and Engineering, Oregon State Univ., Corvallis, OR 97331 (corresponding author). E-mail: rakesh.gupta@oregonstate.edu

[3]Professor, School of Civil and Construction Engineering, Oregon State Univ., Corvallis, OR 97331.

[4]George T. Abell Professor of Infrastructure, Civil and Environmental Engineering, Colorado State Univ., Fort Collins, CO 80525.

[5]Senior Engineer In Training, Hydraulic Design Group, GAI Consultants, Inc., 385 East Waterfront Dr., Homestead, PA 15120.

[6]Senior Faculty Research Assistant, Dept. of Wood Science and Engineering, Oregon State Univ., Corvallis, OR 97331.

Note. This manuscript was submitted on November 9, 2011; approved on July 20, 2012; published online on August 10, 2012. Discussion period open until January 1, 2014; separate discussions must be submitted for individual papers. This paper is part of the ***Journal of Structural Engineering***, Vol. 139, No. 8, August 1, 2013. ©ASCE, ISSN 0733-9445/2013/8-1318–1325/$25.00.

2-story wood-framed residential structure. The structure was impacted with waves and tested in both flooded and nonflooded conditions. The measured forces were mainly uplift forces owing to wave loading and resulting overturning moments. The qualitative analysis of the data showed that differences in structural stiffness throughout the structure will cause a different load distribution in the structure; e.g., overhanging eaves above the garage can provide unanticipated loading conditions, water traveling beneath the structure generates predominantly uplift forces, and the effect of waves breaking on or near the structure greatly increases the loading. The ratio of force from the windows-closed condition to that from the windows-open condition is approximately 2.5:1. Using the results from the one-sixth-scale house, van de Lindt et al. (2009a) developed a base shear-force relationship to wave height.

Arikawa (2009) used a large-scale hydraulic flume to determine the failure mechanisms resulting from impulsive tsunami loads on concrete walls. Based on wave speed and profile, that study also focused on qualitatively dividing surge-front tsunami force into three types: overflow, bore, and breaking. Overflow is defined by a low flood velocity. Bore flow is characterized by quick flow, and the inundated tsunami carries out soliton fission. The third type of force, breaking, occurs when the tsunami breaks in front of the structure; this is seen often when the building is close to the shore or a steep sea bed. Oshnack (2010) used the same wave flume and bathymetry discussed in this paper to examine the tsunami load effects from varying the cross-shore location of a vertical rigid aluminum wall. Robertson et al. (2011) examined the forces from waves propagating on a flooded reef using the same flume bathymetry and aluminum wall as Oshnack. The results were then compared with equations, including the work of Cross (1967), and a new equation was developed for use with flooded reef conditions.

Along with the numerous laboratory experiments to study the effects of tsunamis just discussed, there have been many lessons learned from field reconnaissance. The buildings of the 2004 Indian Ocean Tsunami in Thailand were analyzed by Lukkunaprasit and Ruangrassamee (2008), Ruangrassamee et al. (2006), and Saatcioglu et al. (2006). The hydrodynamic forces from the tsunami were larger than anticipated and exceeded the design wind loads for the coastal buildings. Poor construction and detailing standards also contributed to the substantial structural failures observed during this tsunami.

A special issue of the *Journal of Disaster Research* in December 2009) contained multiple papers that focused on tsunami loading on structures. Arikawa (2009) performed large-scale experiments in Japan investigating the performance of both concrete and wooden walls under impulsive tsunami forces. Most of the work focused on the performance of concrete walls of various thicknesses and did not provide any direct force measurements for wooden walls. Arikawa tested only one wooden wall and eight concrete walls and only provided a sequence of photographs showing the destruction of the wooden wall. Arikawa concluded that the walls would break when a 2.5-m tsunami force hit the walls. Oshnack et al. (2009) evaluated the effectiveness of seawalls in reducing tsunami forces on an aluminum wall, and van de Lindt et al. (2009b) measured lateral force from tsunami bore waves on a one-sixth-scale residential building typical of North American coastal construction. Several authors examined tsunami forces on various structures (Arnason 2005; Arnason et al. 2009; Fujima et al. 2009; Lukkunaprasit et al. 2009).

For the case of uniform steady flow impinging on a vertical boundary, the force per unit width F can be estimated using the conservation of linear momentum (Cross 1967) as

$$F = \tfrac{1}{2}\rho g h^2 + \rho h u^2 \quad (1)$$

where ρ = fluid density; g = gravitational constant; h = water depth of the flow; and u = depth uniform velocity. For the case of a wedge of water with nonuniform flow, Cross (1967) gives

$$F = \tfrac{1}{2}\rho g h^2 \quad + \quad C_f \rho h u^2 \quad (2)$$

where C_f = a force coefficient and can be related to the angle θ made by the leading edge to the dry bed. The force coefficient is small for small angles and varies $1 < C_f < 1.5$ for θ in the range $0 < \theta < 30°$. Comparing with laboratory observations using a 6.9-m-long by 0.15-m-wide glass-walled flume, Cross (1967) found that Eq. (1) adequately predicted the force of surges with surface slopes of $< 10-15°$ and gave some indication that the force coefficient in Eq. (2) should be used to predict the sharp peak resulting from splash-back of water after the initial impact. An objective of this work is to use large-scale tests to evaluate whether Eq. (1) holds for the case of an unsteady bore impinging on a wall or a correction coefficient C_f is needed.

For clarity, because both the maximum force and the quasi-steady force are related to the hydrodynamic conditions for a tsunami bore impinging on a fixed object, the term transient force is used to describe the peak force during the initial bore-structure interaction and quasi-static force is used to describe the force as the bore is reflected from the structure.

Experimental Setup

Wave Flume Bathymetry

The experiments were conducted at the NEES Tsunami Facility in the Large Wave Flume (LWF) at the O. H. Hinsdale Wave Research Laboratory at Oregon State University. The flume is 104 m long, 3.66 m wide, and 4.57 m deep. The flume is equipped with a piston-type wavemaker with a 4-m stroke and maximum speed of 4 m/s, with the capacity of generating repeatable solitary waves. The LWF bathymetry consisted of a 29-m flat section in front of the wavemaker, followed by a 1:12 slope impermeable beach for 26 m, with the rest of the flume consisting of a flat section on a 2.36-m-high false floor. This section will be referred to as the reef to be consistent with other experiments conducted at the O. H. Hinsdale Wave Research Laboratory (e.g., Robertson et al. 2011). The LWF bathymetry is shown in Fig. 1, including the test specimen in relation to the wavemaker.

Flume Instrumentation

The LWF was instrumented (Fig. 1) with 10 wire resistance wave gauges (WGs) and four ultrasonic wave gauges (USWGs) along the flume to measure variations in the instantaneous water surface level as the wave moved inland. These gauges were calibrated at the start of the experiment and when the flume was drained and refilled. WGs 1–10 were placed at x-positions of 17.64, 28.60, 35.91, 40.58, 42.42, 44.25, 46.09, 48.23, 50.37, and 54.41 m with respect to the wavemaker in the zeroed position. USWG 1 was colocated with WG 4 (40.58 m), and this enabled the calibration of the other surface piercing gauges. USWGs 2 and 3 were located at x-positions 54.35 and 58.07 m, respectively. A fourth USWG was located on the movable bridge at x-position 21.50 m. The wavemaker was instrumented with sensors to track the wavemaker x-position and water level on the wavemaker board. The LWF was also equipped with four acoustic-Doppler velocimeters (ADVs) to collect wave-particle velocities at (x, y, z) positions, in meters, of ADV 1 (43.33, −1.10, 1.67), ADV 2 (47.01, −1.08, 1.95), ADV 3 (54.24, −1.28, 2.45), and ADV 4 (57.89, −1.33, 2.45). The locations for these wave

J. Struct. Eng., 2013, 139(8): 1318-1325

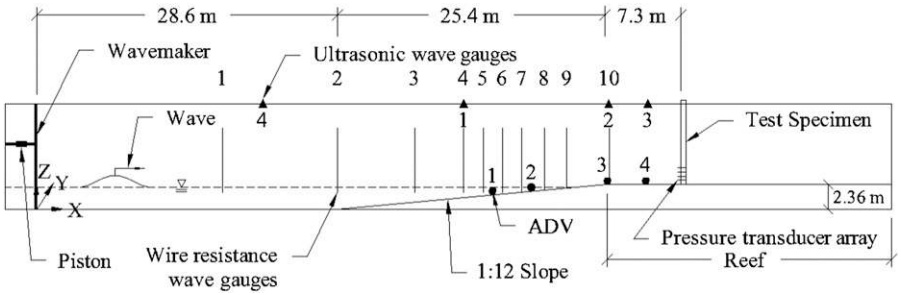

Fig. 1. Elevation view of wave flume with transverse-wall setup

profile and velocity instruments can be found in Fig. 1. The velocity from ADV 4, 0.09 m above the reef, and wave height from USWG 3 were used in calculating Eq. (1) because they were colocated closest to the structure. WG 2 was used to measure the offshore tsunami wave height H_2.

Specimens and Configurations

The test specimens used in these experiments were flexible wood walls built to International Residential Code (International Code Council 2009) standards commonly found in residential and light-commercial construction. During the transverse wood-wall (TW) experiments, three different specimens were used (Table 1). The first specimen used was Specimen 1, a 2×6 (38- $\times$ 140-mm) vertical stud wall sheathed with 13-mm (0.5-in.) five-ply Structural 1 plywood. Two replicates (1A, 1B) of Specimen 1 were built and tested. The wall was 3.58 m (11.75 ft) long and 2.44 m (8 ft) high, having a stud spacing of 40.6 cm (16 in.) on-center. The second wall, Specimen 2, was the same dimensions as Specimen 1 but was made with 2×4 (38- $\times$ 88-mm) dimension lumber instead of 2×6 vertical studs. Two replicates (2A, 2B) of Specimen 2 were built and tested. The last specimen was Specimen 3, which was a 2×6 wall similar to Specimen 1 but with a stud spacing of 61 cm (24 in.) instead of 40.6 cm. Only one Specimen 3 (3A) was built and tested.

All the walls used a nailing pattern of 10.2 cm (4 in.) on-center on edges and 30.5 cm (12 inches) on-center in the field with 8d common nails (63.5 mm long $\times$ 2.87 mm in diameter). Each wall was constructed with Douglas fir kiln-dried No. 2 and better studs and used double end studs.

During the eight different TW tests (Table 2), three different anchorage and load-cell configurations were used. Only the first four experiments are analyzed in this paper because they have similar configurations and allow for comparison with Eq. (1). For experiments TransverseWoodWall_1 (TW 1), TransverseWoodWall_2 (TW 2), and TransverseWoodWall_3 (TW 3), the wall was only anchored to the four horizontal load cells. Fig. 2 shows the wall and load cells, and Fig. 3 shows a schematic diagram of the wall with instrumentation. For the TransverseWoodWall_4 (TW 4) experiment, the bottom sill was anchored to the flume floor with six anchor bolts (1.59 cm in diameter) at distances of 0.41, 1.11, and 1.68 m from the center of the wall. The individual specimen information can be found in Table 1, and a summary of each experiment configuration and specimen used is provided in Table 2.

Wall Instrumentation

The walls were equipped with uniaxial donut-shaped load cells with a capacity of ± 89 kN (± 20 kip). The TWs were equipped with four load cells, one at each corner of the wall (Fig. 2). They were mounted between a metal bracket bolted to the flume wall and a plate attached to the wall. This configuration measured the horizontal forces imposed on the wall during the tsunami event and allowed for comparing the predicted forces from Eq. (1) with the measured forces. Three pressure transducers were also installed on each wall at varying heights. The pressure transducers were mounted to aluminum plates that were then placed into small holes in each wall. The walls were also equipped with two linear variable differential transformers (LVDTs) at the middle of the wall to measure the deflection of the wall at critical locations. The LVDTs were placed at heights of 0.04 (bottom plate) and 2.18 m (top plate) from the bottom of the wall. When the wall was anchored (TW 4), the bottom LVDT was moved up to the midheight of the wall (1.22 m). Fig. 2 shows

Table 1. Specimen Information

Specimens	Stud spacing (cm)	Lumber size (nominal)	Wall length (m)
1A, 1B	40.6	2×6	2.67
2A, 2B	40.6	2×4	2.67
3A	61.0	2×6	2.67

Table 2. Experiment Summary

Experiment	Trials	Wave heights H_2 (m)	Specimen	Anchored	Load cells	Failure
TW 1	12	0.10–0.87	1A	No	4	Yes
TW 2	7	0.10–0.65	2A	No	4	No
TW 3	6	0.20–0.78	3A	No	4	Yes
TW 4	11	0.15–1.04	1B	Yes	4	No
TW 5	11	0.14–0.93	1B	Yes	2 top	No
TW 6	4	0.25–0.68	2B	Yes	4	No
TW 7	4	0.26–0.71	2B	Yes	2 top	No
TW 8	5	0.09–0.48	2B	No	4	Yes

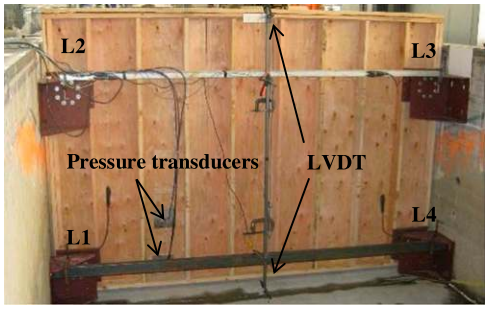

Fig. 2. Transverse-wall instrumentation picture

TW 1 with all the instrumentation. Fig. 3 shows the location of each instrument for a typical TW experiment, and Table 3 summarizes the load-cell and LVDT locations.

Experimental Procedure

Data Acquisition and Processing

Hydrodynamic data (i.e., free surface displacement and velocity) were collected at a sampling rate of 50 Hz. Force, pressure, and displacement data were collected with a sampling rate of 1,000 Hz. The experiment names and trial numbers correspond with those in the experimental notebook supported under the NEES Program of the National Science Foundation. Data from this project can be found on the NEEShub at ⟨http://nees.org/⟩.

Experimental Process

As indicated in Fig. 1, the experiments were performed with a dry reef. When the wavemaker was in the zero position, the water level was set at 2.38 m. The wavemaker was then retracted, causing a decrease in the still-water depth to 2.29 m, referred to as D_o. This gives a depth below the reef of −0.07 m, referred to as D_R. Idealized solitary waves were used to model a tsunami caused by the forward motion of the wavemaker paddle. Because of the finite volume of the flume, this produced a still-water level of approximately +0.03 m above the reef at the end of each run. For each experiment, the wall configuration was tested at an x-position of 61.23 m from the wavemaker. During the eight different TW tests, a total of 60 trials were run with a range of wave heights between 0.09 and 1.04 m. The number of trials, wave heights, specimens used, load-cell configurations, and failures are outlined in Table 2 for each individual experiment.

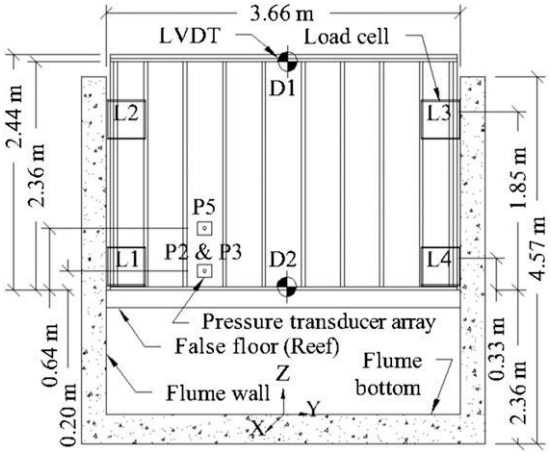

Fig. 3. Typical transverse-wall setup with instrumentation

Table 3. Load-Cell and LVDT Locations

Experiment	Instrument	x (m)	y (m)	z (m)
Load cell (L)				
Transverse walls[a]	L1[b]	61.44	−1.65	0.33
	L2	61.44	−1.65	1.85
	L3	61.44	1.65	1.85
	L4[b]	61.44	1.65	0.33
Linear variable differential transformer (D)				
TWs 1–3 and 8	D1	61.44	0	2.36
(Unanchored)	D2	61.44	0	0.04
TWs 4–7	D1	61.44	0	2.36
(Anchored)	D2	61.44	0	1.22

Note: x-Location is measured from zeroed wavemaker; y-location is measured from center of flume; z-location is from base of test specimen.

[a]Trials 1–6 for initial experiment TransverseWoodWall: locations of L1 and L2 were switched.

[b]Load cells 1 and 4 were removed for experiments TransverseWoodWall_5 and TransverseWoodWall_7.

Unprocessed Data

Fig. 4 shows a portion of the raw data from TW 1 Trial01 tests with $H_2 = 0.29$ m as an example of the hydrodynamic forcing conditions and the structural response. Fig. 4(a) shows the free-surface time series measured at WG 2 at the toe of the slope (Fig. 1), which is used to estimate the offshore tsunami height H_2. Fig. 4(b) shows the free-surface profile of the bore over the reef measured by the third ultrasonic wave gauge (USWG 3) located 3.6 m seaward of the wall, which is used for h in Eq. (1). Fig. 4(c) shows the velocity measured by the fourth ADV (ADV 4) colocated with USWG 3, which used to provide u. Severe signal dropout occurred in the ADV record during the passing of the leading edge as a result of air entrainment. Thus, it

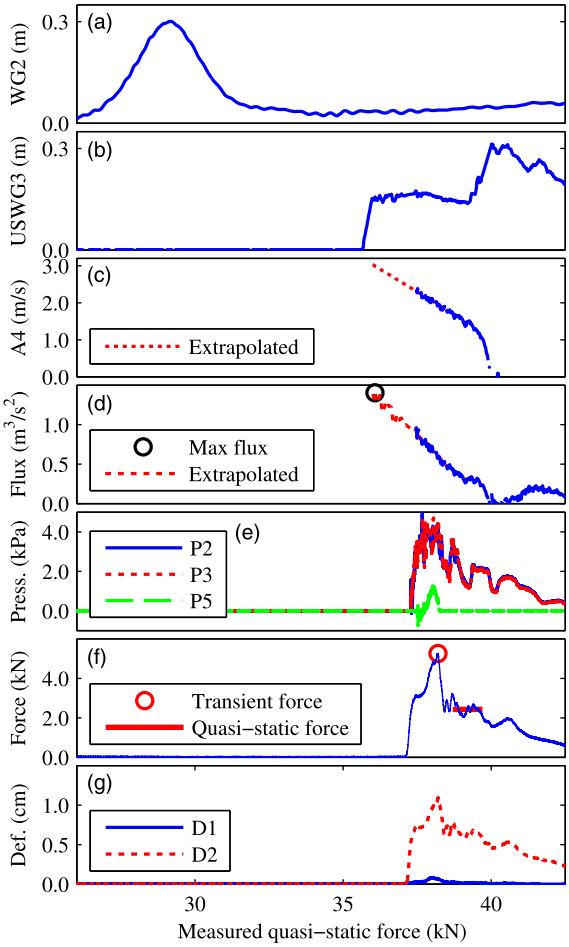

Fig. 4. Example raw-data time history: (a) offshore wave height at WG 2; (b) onshore wave height at USWG 3; (c) velocity at ADV 4; (d) momentum flux at USWG 3 and ADV 4; (e) pressures; (f) total force, transient force, and quasi-static force; (g) deflection

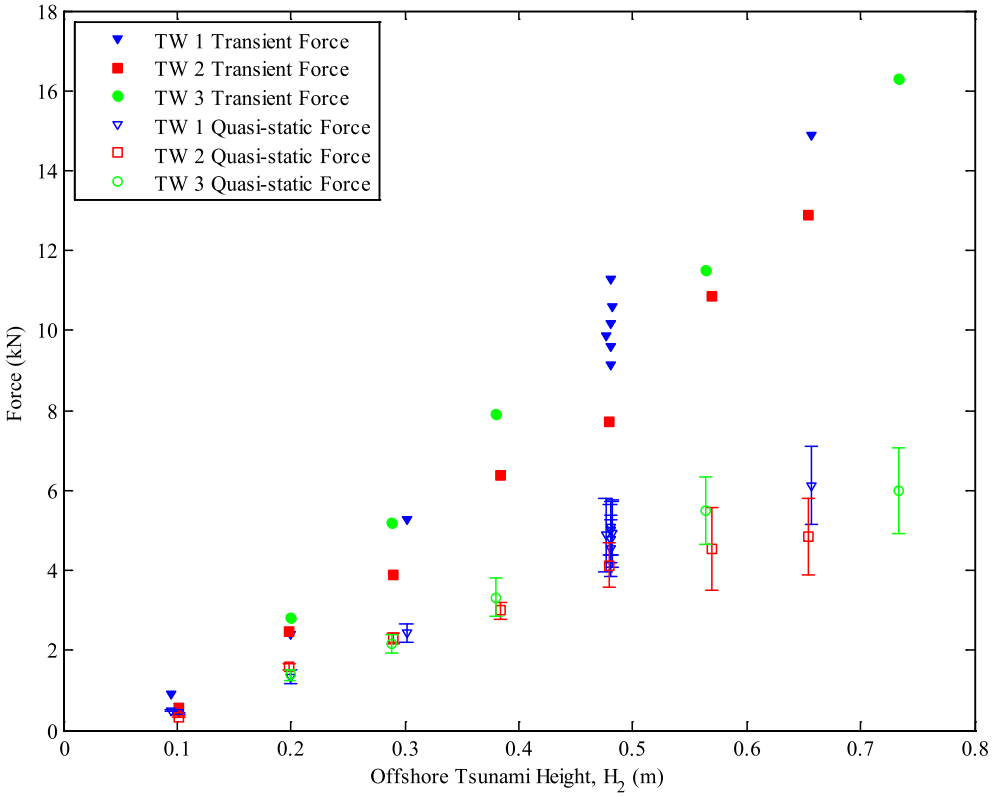

Fig. 5. Transient and quasi-static force comparison for TW 1, TW 2, and TW 3

was necessary to extrapolate the signal back to arrival of the bore indicated by USWG 3. Independent video measurements show that this is a reasonable approximation and that the maximum velocity occurs at the leading edge for this type of flow (Rueben et al. 2011). Use of the extrapolated velocity increased the predicted forces in Eq. (1) by an average of 18%. Fig. 4(d) shows the measured and extrapolated momentum flux per unit width hu^2. Fig. 4(e) shows the pressure measured on the wall. Fig. 4(f) shows the measured total force found by summing the four load cells at each time interval. The transient force (circle) is highlighted as the maximum force in the figure and occurs after the initial impact and is related to the collapse of the water column after impact. The quasi-static force is estimated as the mean of the total force measured for a period of 1.0 s, starting 0.5 s after the peak transient force was observed, and is indicated by a horizontal line. During this time, the bore has reflected from the wall and is propagating back over the reef at a speed slower than the incident bore. It is important to note that no impulsive forces (defined as a sudden, sharp rise in force of short duration during the initial interaction of the bore with the wall) were observed in these tests. Fig. 4(g) shows the deflection of the structure measured by LVDTs along the centerline of the specimen at the top plate (D1, $z = 2.36$ m) and bottom plate (D2, $z = 0.4$ m). These deflection measurements are used to assess the relative performance under transient and quasi-static loads of the different wall assemblies described earlier.

Results and Discussions

Observed Maximum Transient Force and Quasi-Static Force

Fig. 5 shows the measured maximum transient force and average quasi-static force defined in Fig. 4(f) as a function of the offshore

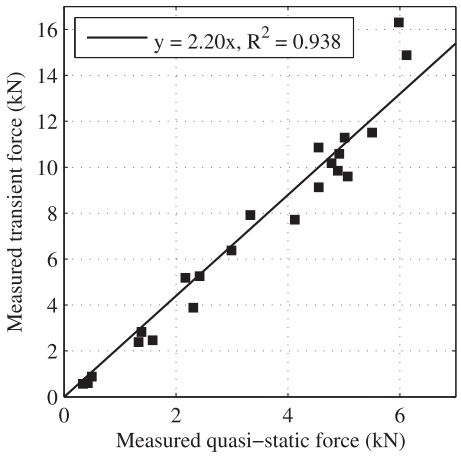

Fig. 6. Measured transient force versus measured quasi-static force

tsunami height H_2 measured at the toe of the slope. It is apparent that both the transient and quasi-static forces increase with offshore tsunami height. The variation in the transient force can be considered linear, although it does not pass through the origin, possibly owing to the inertial effects of accelerating the wall at impact. The variation in the quasi-static force is also linear overall, except possibly for the larger observed wave heights ($H_2 > 0.55$ cm), where there is larger scatter in the data, shown by the large error bars for these points. At $H_2 = 0.50$ cm, more experiments were done to see the repeatability of the experiment. The forces at this level have a coefficient of variation (COV) of 4% and are within a 95% confidence interval, showing that the experiment was repeatable. In any case, it is of interest to compare the relative magnitudes of transient force to

quasi-static force as shown in Fig. 6. For this case, the relationship appears to be linear ($R^2 = 0.938$), with transient force being larger than the quasi-static force by a factor of 2.2 overall.

Comparison with Cross

The predicted forces from Eq. (1) were compared with the measured transient forces. For this comparison, the predicted force per unit width F was multiplied by the breadth of the wall (3.66 m). The maximum momentum flux per unit mass hu^2 was estimated using the extrapolated velocity and the flow depth h from USWG 3. The hydrostatic pressure term in Eq. (1) was calculated using the flow depth corresponding to the maximum momentum flux.

Fig. 7 shows the measured transient force from TW 1, TW 2, and TW 3. These three experiments were chosen because they were unanchored along the bottom sill, so the force from the wave was measured by the four load cells. Trials with small tsunami wave heights ($H_2 \leq 0.1$ m) were excluded because of the poor quality of the ADV data as a result of air entrainment. As can be seen in Fig. 7, Eq. (1) gives reasonable predictions of the peak transient force within an accuracy of about 20%. The force coefficient C_f was calculated using Eq. (2), and the average was found to be $C_f = 0.96$ for this data set. Therefore, from a practical standpoint, it is not necessary to include C_f to obtain reasonable estimates of the transient forces for engineering design. It is noted that although Cross (1967) expressed C_f as a function of the angle of the leading edge, such detailed information about the flow would likely be unavailable for engineering design. The hydrodynamic inputs (i.e., bore height, velocity, and moment flux) are provided in Table 4 along with the measured transient and quasi-static forces.

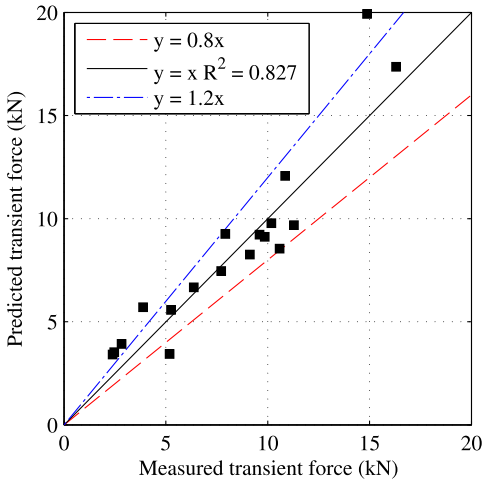

Fig. 7. Predicted versus measured transient force

Wall Performance

For most cases, there were not enough pressure transducers to properly calculate the force. Instead, the pressure transducers were used primarily to show that the pressures were comparable for similar wave heights. Fig. 8 compares the pressure and total force measured on three walls (TW 1, TW 2, and TW 3) with different framing configurations and the same incident tsunami conditions ($H_2 = 0.29$ m). The pressure was taken as the average of P2 and P3 located $z = 20$ cm from the bottom of the wall. For the wall construction, TW 1 and TW 2 had the same stud spacing [40.6 cm (16 in.) on-center], and TW 3 had a larger stud spacing [61.0 cm (24 in.) on-center]. TW 1 and TW 3 used the same dimensional lumber for the studs (2×6 studs), and TW 2 used smaller studs (2×4). All three used the same sheathing [12.6 mm-(0.5-in.) plywood] and bottom sill (2×6). Therefore, it can be said that TW 1 was the stiffest of the three chosen for comparison, and the other two were less stiff because they used smaller studs (TW 2) or greater stud spacing (TW 3). Fig. 8(a) shows that the pressures exerted by the tsunami on the wall were similar, indicating that each wall was subjected to a similar wave loading, with peak pressures at about 4 kPa. The peak transient-force responses were similar for TW 1 and TW 3, indicating that the stud spacing had little effect on the measured peak forces [Fig. 8(b)]. However, the measured forces on TW 2 were lower by about 25% because the smaller studs led to a greater deformation of the wall assembly, thereby lowering the peak force. This reduction in load is only evident during transient force, before stabilizing to a similar quasi-static force as the other two walls. The same trends were observed for the range of wave-height tests for these three wall configurations, with an average transient-force

Table 4. Transient and Quasi-Static Forces with Hydrodynamic Inputs

Experiment	H_2 (m)	h (m)	μ (m/s)	hu^2 (m^3/s^2)	Transient force (kN)	Quasi-static force (kN)
TW 1 Trial01	0.30	0.157	2.990	1.402	5.25	2.42
TW 1 Trial02	0.48	0.204	3.176	2.053	9.12	4.55
TW 1 Trial03	0.48	0.201	3.262	2.137	10.59	4.92
TW 1 Trial04	0.48	0.185	3.568	2.352	9.60	5.07
TW 1 Trial05	0.66	0.219	4.873	5.208	14.88	6.12
TW 1 Trial08	0.48	0.173	3.806	2.498	11.29	5.01
TW 1 Trial09	0.48	0.210	3.289	2.274	9.85	4.89
TW 1 Trial10	0.48	0.205	3.470	2.466	10.18	4.78
TW 1 Trial15	0.20	0.140	2.441	0.836	2.39	1.33
TW 2 Trial02	0.20	0.158	2.308	0.841	2.47	1.58
TW 2 Trial03	0.29	0.160	2.990	1.433	3.88	2.31
TW 2 Trial04	0.38	0.163	3.225	1.692	6.38	2.99
TW 2 Trial05	0.48	0.161	3.447	1.911	7.72	4.12
TW 2 Trial06	0.57	0.192	4.028	3.118	10.86	4.55
TW 3 Trial01	0.29	0.096	3.044	0.893	5.19	2.17
TW 3 Trial02	0.20	0.162	2.414	0.944	2.83	1.38
TW 3 Trial03	0.38	0.169	3.765	2.390	7.92	3.33
TW 3 Trial05	0.73	0.248	4.231	4.442	16.31	5.98

J. Struct. Eng., 2013, 139(8): 1318-1325

reduction in TW 2 of about 18%. This is a significant reduction in the forces that would be subsequently transferred to the rest of the structural systems when part of a building.

This reduction in transient force could be in direct relation to the flexibility of each wall. Fig. 9 shows the maximum deflection at $z = 2.36$ m, the top plate, and $z = 0.04$ m, the bottom plate, along the centerline of the wall as a function of the offshore tsunami height. The overall deflections of both the top and bottom plates are larger for TW 2 (square symbols). The increased flexibility of the 2×4 wall shown by higher deflections compared with the stiffer 2×6 walls allows for dampening of the initial impact of the wave. This, in turn, reduces the transient forces on the wall. It should be noted that although the 2×4 wall was shown to reduce the transient force, the wall failed at a smaller wave height ($H_2 = 0.65$ m) than the similar 2×6 wall because the 2×4 wall's flexural capacity was lower. Although the forces on the overall system were reduced by the 2×4 wall because of lower strength capacity, 2×6 construction should be used in tsunami zones.

The three transverse walls analyzed earlier show a good trend between wall flexibility and transient forces on each wall. However, these walls were unanchored along the bottom plate, which is an uncommon scenario in standard building construction. Fig. 10 shows the complete failure of the bottom plate during Trial16 of the unanchored wall test (TW 1) with a measured offshore wave height H_2 of 0.87 m. This failure was observed because the impact of the wave exceeded the bending capacity of the bottom sill plate (2×6 dimensional lumber, nominal capacity 1,700 N-m). It is important to note that this bending failure likely will not occur if the bottom plate is anchored in typical residential construction standards, as shown in later tests. When the bottom plate was anchored to the flume floor during TW 4, this bending failure was no longer seen. The unanchored wall failed at a small wave height, whereas the anchored wall was not tested to failure because the physical limitations of the facility had been reached.

Summary and Conclusions

In this study, a series of idealized large-scale two-dimensional tsunami wave tests were performed on light-frame wood walls used in typical coastal construction. The following can be concluded based on the work presented in this paper:

1. Transient forces were generated by the impact of the bore on a wall shortly after the initial impact. This was followed by a quasi-static force after the bore reflected from the structure. No impulsive forces were observed for these tests.
2. The ratio of the peak transient force to the mean quasi-static force was 2.2 overall.
3. Eq. (1) from Cross (1967) gives a good estimate of the measured peak transient force within about 20% uncertainty, and it was not necessary to include the momentum correction coefficient C_f in Eq. (2).
4. The standard of construction can affect the peak transient force experienced by the wall by approximately 20% for the three types of construction considered here. This reduced peak transient force would either be transferred to other parts of the building system or would contribute to permanent deformation of the wall and ultimately failure.
5. The quasi-static forces were similar for the three different wall specimens.

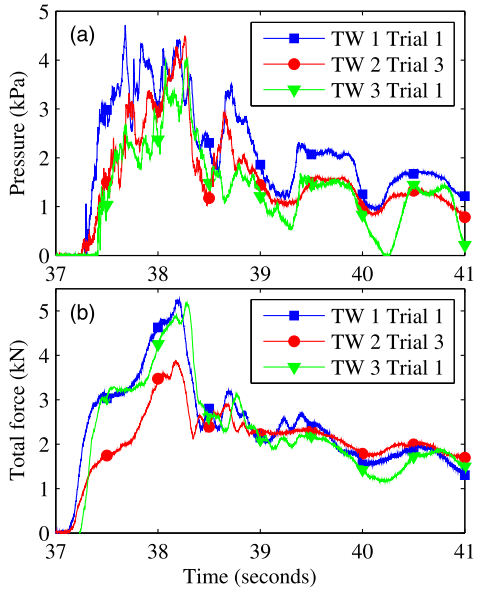

Fig. 8. Pressure (a) and total-force (b) comparisons for TWs 1–3 ($H_2 = 0.29$ m)

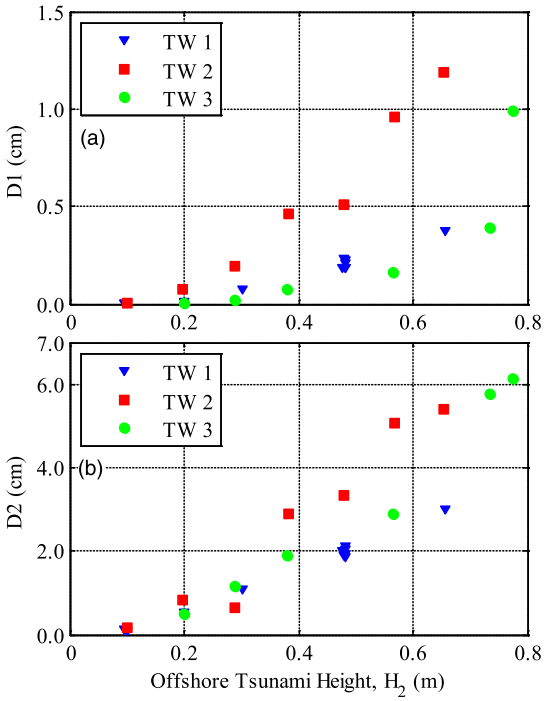

Fig. 9. Deflection D1 (a) and D2 (b) comparison for TWs 1–3

Fig. 10. Failed bottom plate of TW 1 (unanchored, Specimen 1A)

J. Struct. Eng., 2013, 139(8): 1318-1325

6. The controlling failure of the unanchored walls was bending of the bottom plate.

This study represents a significant step toward understanding the complex nature of wave-structure interaction and the performance of light-frame wood construction often used in residential and light-commercial buildings. By better understanding the failure modes of a wood wall during a tsunami event, building designs can be improved to better protect life safety and mitigate costly damage; however, occupants of light-framed residences should be encouraged to evacuate when there is a tsunami warning in effect. Further research is necessary to investigate the effects of openings, three-dimensional flow, and plan irregularities on stress and load concentrations within a more complex structural system.

Acknowledgments

This research was supported by the National Science Foundation under Grant No. CMMI-0530759. The tsunami facility is supported in part by the George E. Brown, Jr. Network for Earthquake Engineering Simulation (NEES) Program of the National Science Foundation under Award No. CMMI-0402490. The authors also thank the O. H. Hinsdale Wave Research Laboratory staff for their invaluable support.

References

Arikawa, T. (2009). "Structural behavior under impulsive tsunami loading." *J Disaster Res.*, 4(6), 377–381.

Arnason, H. (2005). "Interactions between an incident bore and a free-standing coastal structure." Ph.D. dissertation, Univ. of Washington, Seattle.

Arnason, H., Petroff, C., and Yeh, H. (2009). "Tsunami bore impingement onto a vertical column." *J. Disaster Res.*, 4(6), 391–403.

Cross, R. (1967). "Tsunami surge forces." *J. Wtrwy. and Harb. Div.,* 93(4), 201–231.

Fujima, K., Achmad, F., and Shigihara, Y. (2009). "Estimation of tsunami force acting on rectangular structures." *J. Disaster Res.*, 4(6), 404–409.

International Code Council. (2009). *2009 International residential code for one- and two-family dwellings*, Country Club Hills, IL.

Lukkunaprasit, P., and Ruangrassamee, A. (2008). "Building damage in Thailand in the 2004 Indian Ocean tsunami and clues for tsunami-resistant design." *IES J. Part A: Civil & Struct. Eng.*, 1(1), 17–30.

Lukkunaprasit, P., Thanasisathit, N., and Yeh, H. (2009). "Experimental verification of FEMA P646 tsunami loading." *J. Disaster Res.*, 4(6), 410–418.

Oshnack, M. E. (2010). "Analysis of wave forces on prototype walls under tsunami loading." M.S. thesis, Oregon State Univ., Corvallis, OR.

Oshnack, M. E., Aguiniga, F., Cox, D., Gupta, R., and van de Lindt, J. (2009). "Effectiveness of small onshore seawall in reducing forces induced by tsunami bore: Large scale experimental study." *J. Disaster Res.*, 4(6), 382–390.

Ramsden, J. (1996). "Forces on a vertical wall due to long waves, bores, and dry-bed surges." *J. Waterway, Port, Coastal, Ocean Eng.*, 122(3), 134–141.

Robertson, I. N., Riggs, R. H., and Mohamed, A. (2011). "Experimental results of tsunami bore forces on structures." *Proc., 30th Int. Conf. of Ocean, Offshore and Arctic Engineering*, ASME, New York.

Ruangrassamee, A., Yanagisawa, H., Foytong, P., Lukkunaprasit, P., Koshimura, S., and Imamura, F. (2006). "Investigation of tsunami-induced damage and fragility of buildings in Thailand after the December 2004 Indian Ocean tsunami." *Earthq. Spectra*, 22(S3), 377–401.

Rueben, M., Holman, R., Cox, D., Killian, J., and Stanley, J. (2011). "Optical measurements of tsunami inundation through an urban waterfront modeled in a large-scale laboratory basin." *Coast. Eng.*, 58(3), 229–238.

Saatcioglu, M., Ghobarah, A., and Nistor, I. (2006). "Performance of structures in Thailand during the December 2004 great Sumatra earthquake and Indian Ocean tsunami." *Earthq. Spectra*, 22(S3), 355–375.

Thusyanthan, N., and Madabhushi, S. (2008). "Tsunami wave loading on coastal houses: A model approach." *Proc. Inst. Civil Eng.*, 161(CE2), 77–86.

van de Lindt, J., Gupta, R., Cox, D. T., and Wilson, J. (2009a). "Wave impact study on a residential building." *J. Disaster Res.*, 4(6), 419–426.

van de Lindt, J. W., Gupta, R., Garcia, R., and Wilson, J. (2009b). "Tsunami bore forces on a compliant residential building model." *Eng. Struct.*, 31(11), 2534–2539.

Wilson, J., Gupta, R., van de Lindt, J., Clauson, M., and Garcia, R. (2009). "Behavior of a one-sixth scale wood-framed residential structure under wave loading." *J. Perform. Constr. Facil.*, 23(5), 336–345.